Published in "Arteriosclerosis, Thrombosis, and Vascular Biology
31: 2836-2844, 2011" which should be cited to refer to this work.

http://doc.rero.ch

Decrease in VEGF Expression Induces Intussusceptive Vascular Pruning

Ruslan Hlushchuk, Martin Ehrbar, Philipp Reichmuth, Niklas Heinimann, Beata Styp-Rekowska, Robert Escher, Oliver Baum, Philipp Lienemann, Andrew Makanya, Eli Keshet, Valentin Djonov

Objective—The concept of vascular pruning, the "cuting-off" of vessels, is gaining importance due to expansion of angio-modulating therapies. The proangiogenic effects of vascular endothelial growth factor (VEGF) are broadly described, but the mechanisms of structural alterations by its downregulation are not known.

Methods and Results—$VEGF_{165}$-releasing hydrogels were applied onto the chick chorioallantoic membrane on embryonic day 10. The hydrogels, designed to completely degrade within 2 days, caused high-level VEGF presentation followed by abrupt VEGF withdrawal. Application of VEGF resulted in a pronounced angiogenic response within 24 hours. The drastic decrease in level of exogenous VEGF-A within 48 hours was corroborated by enzyme-linked immunosorbent assay. Following this VEGF withdrawal we observed vasculature adaptation by means of intussusception, including intussusceptive vascular pruning. As revealed on vascular casts and serial semithin sections, intussusceptive vascular pruning occurred by emergence of multiple eccentric pillars at bifurcations. Time-lapse in vivo microscopy has confirmed the de novo occurrence of transluminal pillars and their capability to induce pruning. Quantitative evaluation corroborated an extensive activation of intussusception associated with VEGF withdrawal.

Conclusion—Diminution of VEGF level induces vascular tree regression by intussusceptive vascular pruning. This observation may allude to the mechanism underlying the "normalization" of tumor vasculature if treated with antiangiogenic drugs. The mechanism described here gives new insights into the understanding of the processes of vasculature regression and hence provides new and potentially viable targets for antiangiogenic and/or angio-modulating therapies during various pathological processes.

Key Words: angiogenesis ■ morphogenesis ■ vascular biology ■ intussusceptive vascular pruning

The inaugural capillary plexus of any vascular network undergoes substantial remodeling for the vasculature to meet the needs of the developing organ and to establish the organ-specific angio-architecture.[1,2] Vascular pruning is an essential adaptive mechanism resulting in regression of excessive vascular branches and creation of hierarchical, thermodynamically efficient angioarchitecture. This process has been known for many decades; in 1873 Roguet nicely illustrated this important phenomenon and named it "retraction of capillaries."[3] In 1961 Ashton stated that retraction of capillaries plays a key role in the reorganization of the primitive immature capillary network.[4] It was considered that some channels become redundant, blood flow within them ceases, the lumen obliterates, and the endothelial cytoplasm and nuclei retract into the parent capillaries leaving behind a trail of cytoplasm that disappears.[5] This was the first profound description of a mechanism of vascular pruning at capillary level.

In the recent past, the understanding of vascular remodeling has been substantially improved, partially, through detailed investigations and descriptions of the process of intussusceptive angiogenesis, and in particular, intussusceptive vascular pruning (IVP).[1,6,7] Our previous morphological studies have revealed the vasculature of different organs to undergo 2 main phases of development: an early sprouting phase followed by an intussusceptive phase, during which capillary sprouting is superseded by transcapillary pillar formation. Intussusception results in rapid expansion of the capillary network and the genesis of an organ-specific vascular tree, as well as its dynamic adaptation and intussusceptive branching remodeling (see review[1]). An important facet of intussusception is the IVP. It can be summarized as the formation of multiple eccentric pillars at the bifurcation points and their subsequent successive fusions, which leads to partial and later to total luminal obstruction and separation (cutting-off) of one of the affected daughter branches. The

From the Institute of Anatomy (R.H., P.R., N.H., B.S.-R., A.M., V.D.), University of Fribourg, Fribourg, Switzerland; Department of Obstetrics (M.E., P.L.), University Hospital of Zurich, Zurich, Switzerland; Institute of Anatomy (R.H., B.S.-R., V.D.), University of Bern, Bern, Switzerland; Hadassah Hebrew University School of Medicine (E.K.), Hebrew University, Jerusalem, Israel; Inselspital (R.E.), University Hospital of University of Bern, Bern Switzerland.

R.H. and M.E. contributed equally to this work.

Correspondence to Valentin Djonov, MD, Institute of Anatomy, University of Bern, Baltzerstrasse 2, Bern 3012, Switzerland. E-mail valentin.djonov@ana.unibe.ch

latter mechanism is alternative to the one described by Ashton and, in contrast, it is not limited to the capillary level but also involves larger vessels. Vascular pruning results in reduction of the number of vascular branches and vascular density respectively. This is one of the mechanisms allowing the vascular system to dynamically adapt to the changing hemodynamical and metabolic influences and to create mature hierarchical and even more efficient angioarchitecture.[8]

The remodeling process is regulated by mechanical influences (hemodynamics), as well as by numerous not yet well-defined morphogens and cytokines. The most potent and best known angiogenic factor, vascular endothelial growth factor (VEGF)-A, plays a major regulatory role in the formation of blood vessels and is known to control proliferation and migration of endothelial cells.[8–10] Proliferation of endothelial cells is regulated by absolute concentration of VEGF, whereas their migration and differentiation toward different functionalities depends on the concentration gradient of different VEGF-isoforms.[11,12] VEGF also influences the survival of vascular endothelial cells.[9] Our ongoing studies in the developing kidney revealed the relation between VEGF downregulation and intussusceptive pruning (A. Makanya et al, unpublished data). The sustained VEGF expression or, respectively, its inhibition was shown to play an important role in vascular remodeling.[13,14] The finding by Keshet's group that VEGF is the molecular link between hypoxia and angiogenesis was a milestone in the field of hypoxia-driven angiogenesis.[15] In a previous study we demonstrated that inhibition of VEGF/VEGF-R signaling pathway led to vessel degeneration in the chick chorioallantoic membrane (CAM), most probably by means of vascular pruning.[16] Moreover, in a recent study we described how application of a VEGF inhibitor in the mouse xenografts tumor model led to a temporary switch in the angiogenesis mode: from sprouting to intussusception.[14] The described findings underpin the paramount role of VEGF (or actually its inhibition) in activation of intussusceptive angiogenesis, and, in particular, IVP.

In the present study we have investigated one of the possible regulatory mechanisms underlying intussusceptive angiogenesis, the one involving VEGF-signaling pathways. We show here that IVP is preceded by a reduction of available VEGF. We have described the morphogenesis of IVP and discussed the biological and clinical relevance of this fundamental vascular process.

Materials and Methods

Local Application of VEGF-A

A 1.0 μg recombinant VEGF-A_{165} protein (Peprotech, London) was administered in a 10 μL 2% (weight /Volume) synthetic fibrin analog hydrogel. The hydrogels were formed under physiological conditions by enzymatic cross-linking of 8-arm star-shaped poly (ethylene glycol) PEG polymers, which are functionalized with substrate sequences for FXIIIa as previously described.[17] Hydrogels without addition of VEGF-A_{165} were used as vehicle controls. In order to facilitate the localization of the applied hydrogel and estimate the level of its degradation on the CAM in some experiments FITC-labeled peptides Lys-FITC (Ac-FKGGK-fluorescein-NH_2, NeoMPS, Strasbourg, France), which are covalently tethered to the forming hydrogels, were added.

Intravital Microscopy of CAM Vasculature

Chorioallantoic membranes were obtained by incubating chick embryos using the established shell-free culture method.[18] On E10 portions of the CAM surface were treated with hydrogels that either contained or did not contain 1 μg of VEGF-A_{165}. Twenty four, 48, and 72 hours after the application, the CAMs were intravenously injected with up to 0.1 mL of 3% FITC-dextran solution [molecular weight: 2′000′000 Da (Sigma, Buchs, Switzerland)], prior to inspection in an epifluorescence microscope (Polyvar-Reichert, Glattbrugg, Switzerland) equipped with a Canon 5D Mark II camera for both video recording and taking of still images. The still images and video sequences of at least 4 fields of view were taken per application site for further quantitative evaluation. The total number of branching points per field of view was assessed using analySIS Software 5.0 (Soft Imaging System, Muenster, Germany) by means of user-driven skeletonization of the vasculature.

The Multiple Image Alignment tool of the aforementioned software was used to obtain overview images representing the whole application site with degrading gel at different timepoints. In cases where the applied gels contained FITC labeled peptides, we injected up to 0.1 mL of 3% Rhodamine B isothiocyanate dextran solution [molecular weight: 70′000 Da (Sigma, Buchs, Switzerland)] in isotonic NaCl solution.

Determination of Remaining VEGF by Enzyme-Linked Immunosorbent Assay

We harvested and homogenized 1 cm^2 sized CAM samples from the site of treatment (including remaining hydrogel mass) in 500 μL lysis buffer (PBS pH 7.2, 0.1% Tween, 0.2% BSA, 1 mmol/L Benzamidine, 20 mmol/L NaF, 1 mmol/L PMSF, 2% Protease Inhibitor Cocktail Set III [Calbiochem, Darmstadt, Germany]) and incubated for 24 hours at 4°C on a rotating wheel. VEGF-A_{165} content in the lysis buffer was assessed using a human VEGF enzyme-linked immunosorbent assay (ELISA; PeproTech, London, UK) according to the manufacturer's protocol.

Semithin Serial Sectioning

CAM samples of sites of interest were harvested and fixed in 2.5% (v/v) glutaraldehyde solution buffered with 0.03 mol/L potassium phosphate (pH 7.4, 370 mOsm). They were then postfixed in 1% OsO_4 [buffered with 0.1 mol/L sodium cacodylate (pH 7.4, 340 mOsm)], dehydrated in ethanol, and embedded in epoxy resin. Thousands of 0.8-μm–thick serial sections were prepared using glass knives and stained with Toluidine Blue. The serial sections were viewed and images captured at low magnification using a light microscope (Leica, Leitz DM), equipped with Leica DFC480 camera. The set of images obtained was aligned using Adobe Photoshop CS3 Software and imported as stacks into Imaris Software for low resolution 3D-reconstruction. The ensuing 3D data enabled exact localization of the branching points of interest based on direct comparison with the in vivo microscopy images of corresponding sites. Then images of the defined sections were taken at high magnification ($\times$1000) and the site of interest was reconstructed at high resolution by using the procedure described above.

Vascular Casting

Vascular casts were prepared as previously described.[19] Briefly, CAM vasculature was perfused with a freshly prepared solution of Mercox® (Vilene Company, Japan) containing 0.1 mL of accelerator per 5 mL of resin. One hour after perfusion, the CAM were transferred to 7.5% potassium hydroxide for dissolution of tissue, which was effected over a course of 2 to 3 weeks. After washing, the casts were dehydrated in ethanol and dried in a vacuum desiccator. The samples were then sputtered with gold to a thickness of 10 nm and examined in a Philips XL-30 SFEG scanning electron microscope.

Index of Intussusception and Statistical Analysis

From video sequences the number of branching points involved in intussusception (ie, those showing pillars) could be assessed. The

http://doc.rero.ch

http://doc.rero.ch

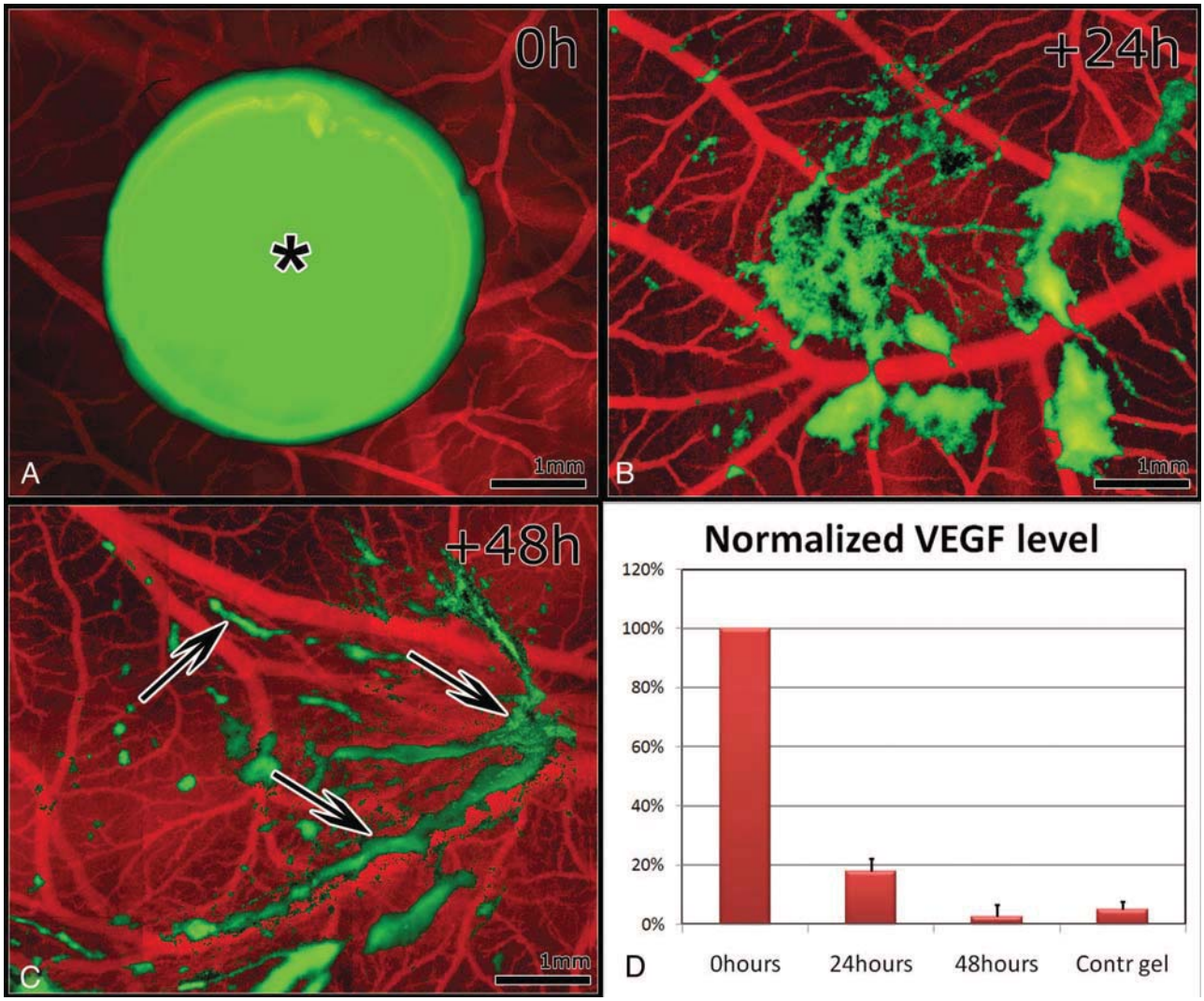

Figure 1. Hydrogel based delivery of vascular endothelial growth factor (VEGF). An overview of gel (asterisk) just after its application on an E10 CAM is presented in **A**. In the background the vascular network was visualized by intravenous injection of RITC-dextran. At 24 hours after the application (**B**) the amount of gel was remarkably reduced. At 48 hours (**C**) only traces of the gel (arrows) could be detected. The graph showing the normalized VEGF levels obtained by ELISA is presented in **D** (mean values± SD; n=3). Contr indicates control.

vasculature skeletons on the corresponding still images were used to find out the total number of branching points per each investigated field of view. By dividing the number of intussusception involved branching points by the number of branching points, the index of intussusception could be determined. At least 4 fields of vision per application site were evaluated (n=4 per time point and per group, at least 16 fields of vision per time point and group) The used magnification was ×40. Statistical analysis was done using the 2-tailed *t* test. The difference was considered significant if $P<0.05$.

Apoptosis Assay

Apoptotic cells were detected in vivo using Annexin V-FITC apoptosis detection kit (Sigma-Aldrich Chemie GmbH, Steinheim, Germany). The solution was injected directly into the CAM vascular system. After 15 minutes of incubation the vasculature was examined using a Leica AF 6000LX fluorescence microscope equipped with the Leica DFC 360FX digital camera. Annexin V-positive (=apoptotic) cells appeared as green spots in the images obtained.

Results

VEGF Release Profile

An angiogenic response was stimulated by local application of gels loaded with 1 μg of VEGF or empty gels (control) on top of growing chick CAM at E10. To allow the estimation the VEGF release profile we have added Lys-FITC to the gel composition. The FITC labeling of the hydrogel enabled the visual presentation of the proteolytic gel degradation and allowed the correlation of proteolysis-triggered release of VEGF with the amount of the remaining hydrogel mass[20] (Figure 1). Another advantage of this application method is that removal of the gel after certain application time was not necessary in our experiments, avoiding the very often observed nonspecific reactions of the CAM vasculature due to mechanical damage or irritation.[21] The gel was considerably degraded as early as 24 hours and completely degraded in 48

hours after the application (Figure 1A–1C) and no more detectable at later time-points (data now shown).

Determination of the VEGF-A levels using ELISA-kit has corroborated that the amount of exogenous VEGF-A remained at a significantly higher level at 24 hours when compared to controls. At 48 hours VEGF expression decreased back to the level in control samples (Figure 1D).

Thus, in our model an exhaustive stimulation by exogenous VEGF was achieved for more than 24 hours followed by a drastic drop in VEGF levels by 48 hours.

Morphogenesis of IVP

In order to investigate the detailed morphology of the affected vasculature we made vascular corrosion casts of CAMs at 24 and 48 hours after VEGF application. Observation of casts using scanning electron microscope corroborated the hypothesis that besides the differences between control (Figure 2a) and VEGF-treated samples, there was a qualitative change between the vasculature during VEGF stimulation (at 24 hours) (Figure 2B) and when the VEGF presentation was discontinued, namely at 48 hours (Figure 2C–2H). In the latter ones there were numerous bifurcations involved in IVP. Various stages of the pruning process were documented on vascular casts made at 48 hours after VEGF-A application (Figure 2C–2H). Initially single eccentrically positioned pillars (arrowheads in Figure 2) arise (Figure 2C–2D), they then grow in number and girth (Figure 2D), and folds (arrows in Figure 2) emerge between them (Figure 2E–2F). As the folds become deeper (Figure 2F–2G), pillars fuse and finally lead to the "cutting-off" of the corresponding vessel branches (Figure 2G). These changes take place simultaneously in a "cascade-like" manner at many branching levels, from capillary plexuses up to larger vessels (Figure 2H). Note the IVP-altered capillary plexus indicated with an asterisk in Figure 2H.

Apparently, IVP was activated 48 hours after VEGF-A application, soon after the dramatic decrease in VEGF-A expression.

Time Course of IVP

Time-lapse in vivo video microscopy (Figure 3) confirmed the aforementioned activation of IVP following VEGF-A downregulation by revealing the appearance of many asymmetrically positioned pillars, the hallmarks of intussusceptive pruning. The fast appearance and progression of the pillars (within hours) enabled the documentation of various stages of IVP in vivo: from appearance of single eccentrically positioned pillars to formation of pillar rows (Figure 3A–3C) and almost complete "cutting-off" of the daughter vessel with drastic decrease in the size of its orifice resulting in the vessel being hardly patent. The same fate befell the neighboring capillary plexus (Figure 3D–3F). The corresponding vascular cast image with multiple intussusception involved branching and, due to pruning altered capillary plexus, is presented in Figure 2H.

These findings illustrate the rapid change in vascular structure accomplished by intussusception.

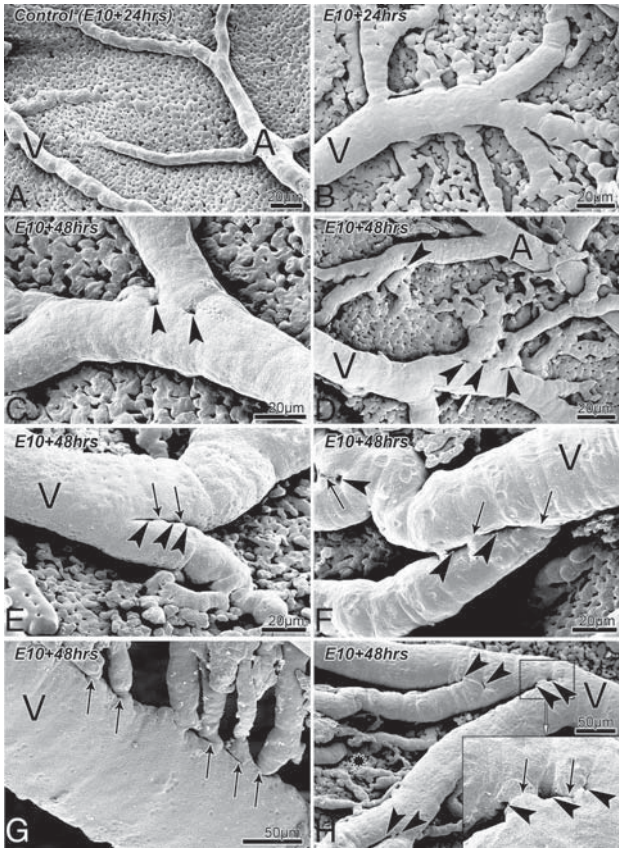

Figure 2. Intussusceptive vascular pruning revealed by vascular casting technique. Control CAMs showing a regular vascular network with an intact capillary plexus between artery (A) and vein (V) (**A**). The vascular casts made at 24 hours post-application displayed the angiogenic stimulation (**B**) with a dense tree of enlarged feeding vessels and numerous side branches. At 48 hours after application there was a remarkable activation of intussusception at the branching points (**C–H**). Unlike the controls, in the VEGF-treated sites asymmetrically positioned pillars (arrowheads in [**C–H]**) or connecting folds (arrows in **E–H**) were frequent findings. Various stages of the pruning process were found: where pillars grow in girth and number (**C** and **D**), fuse by growing folds (arrows) and lead to subsequent "cutting-off" of the corresponding vessel branches (**E–G**). The simultaneous "cascade-like" intussusceptive pruning at different hierarchical levels of venous tree is presented in **H**. The larger vessels as well as the capillary plexus (asterisk) are altered. The insert in **H** shows the asymmetrically positioned pillars (arrowheads) and the folds between them (arrows).

High Resolution 3D-Reconstruction Using Serial Semithin Sectioning

The branching point of interest with emerging pillars observed in vivo (Figure 4A–4C) was fixed just after the last in vivo observation and then processed for semithin sectioning. Over 2000 serial 0.8 μm-thick sections were made with the cutting plane being perpendicular to the CAM surface and stained with toluidine blue. Low magnification images of these sections were acquired, aligned, and processed for low resolution 3D-reconstruction using Imaris Software. The data obtained by 3D-reconstruction was used for precise localization of the vascular segment of interest (white rectangle in Figure 4C) by superimposing it with the in vivo images. Afterward high magnification images of determined sites in 140 sections were acquired for high resolution 3D-

http://doc.rero.ch

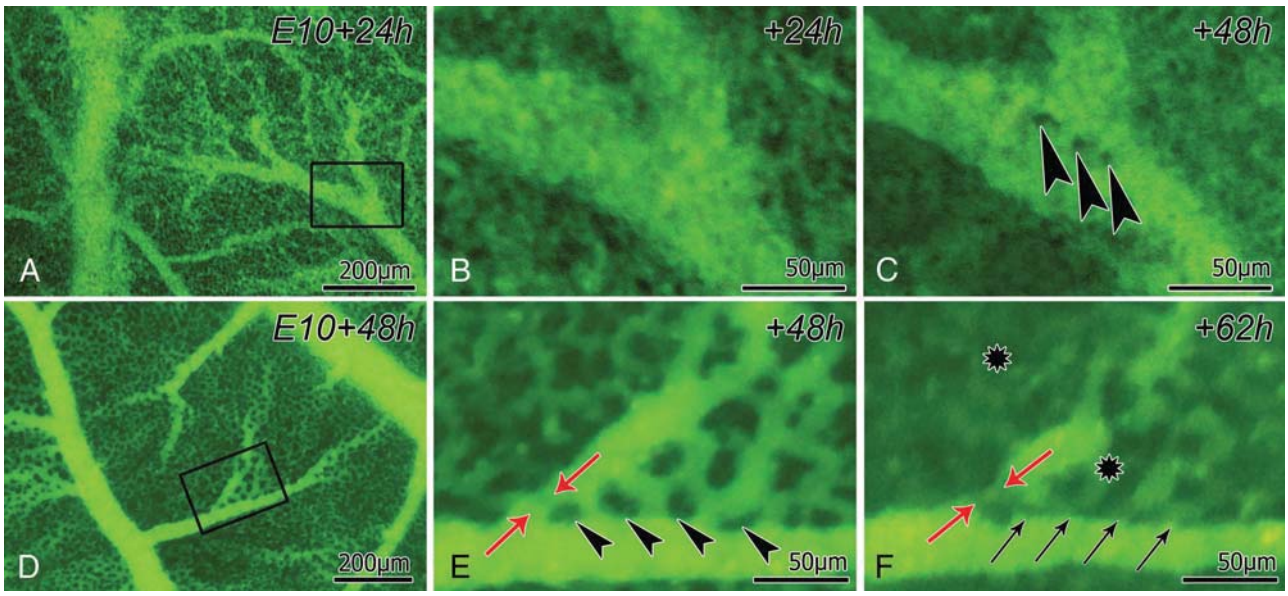

Figure 3. Time-lapse in vivo microscopy at 24 (**A**, **B**), 48 (**C–E**) and 62 (**F**) hours after vascular endothelial growth factor (VEGF) gel application. **A–C**: The branching of interest (rectangle in **A**) is presented at higher magnification in **B** and shows no signs of intussusceptive pruning at 24 hours after VEGF-A application. The pillars (arrowheads in **C**) emerged within the next 24 hours and were aligned in a row at the origin of one of the daughter vessels. A more advanced stage of vascular pruning is presented in **D–F**: The branching of interest marked in **D** is presented at higher magnification in **E**. The branching undergoes intussusceptive pruning at 48 hours after VEGF-A application: Rather large pillars (arrowheads in **E**) separate the daughter vessel. After another 14 hours the pillars further increased in size decreasing the orifice of the daughter vessel (red arrows in **E** and **F**) and making it and neighboring capillary plexuses (asterisks in **F**) barely patent. Arrows in **F** point at the disappearing connections to the capillary plexus which correspond to the rows of folds as displayed in Fig. 2G. **F** corresponds to image of vascular cast in Fig. 2G and 2**C** to the one in Fig. 2E.

http://doc.rero.ch

reconstruction: the virtual section through the 3D-stack is presented in Figure 4D. Further, the 3D surface of the vascular lumen of the in vivo segment of interest was computer generated (Figure 4e) and corresponded to the in vivo obtained images (see Figure 4C for comparison). The intraluminal view demonstrates clearly that the structures observed in vivo were emerging pillars (Figure 4F). On the corresponding semithin sections, the intraluminal protrusions of endothelial cells at the opposing sides of the vascular lumen were apparent (Figure 4G–4H).

Adaptation (Regression) of the Vasculature Happens at Different Hierarchical Levels, and Including Larger Supplying Vessels

At 72 hours after VEGF application even the usually rigid larger arteries also underwent the intensive process of adaptation (Figure 5). Intussusceptive pruning and remodeling was not restricted to distal part of vasculature but could be observed along the entire vascular tree (Figure 5B–5D). This presents the integrity of the vasculature system adaptation and involvement of intussusception in the regressive remodeling at all hierarchical levels of the vasculature.

Morphometry of the Affected Vasculature

Quantification of intussusception was done using the data obtained using in vivo microscopy. The parameter we have chosen as the measure of intussusception was the index of intussusception involved branching points. The results obtained have corroborated the qualitative description: In the control areas, there were no significant changes of this parameter at all 3 time-points. On contrary, the VEGF-A treated areas were characterized by a constant increase of intussusception involved branching points with the most prominent value (>2.5fold in comparison with control) at 72 hours (Figure 6).

Apoptosis of Endothelial Cells at Remodeled Sites

To address the question whether the endothelial cells undergo apoptosis we made the additional experimentation: The IV injection of FITC-labeled anti-Annexin–V apoptosis detection kit was made prior in vivo observation of the VEGF application sites. The apoptotic cells could be found at 48 hours and more after the application. At E10+48 hours there were scattered apoptotic cells in the capillary plexus and at E10+72 hours one could observe already bigger vessels with numerous Annexin-V–positive cells (see Figure 7).

Discussion

Mechanism of Vascular Pruning

The mechanism of IVP has been rather explicitly described in the last decade.[6,22] At the initial stage intraluminal protrusions of endothelial cells lying at the opposing sides of the vessel are formed. The contact between them has to be established for the single pillar to emerge. The peculiarity of IVP is that the pillars are positioned eccentrically from the axis of the mother vessel. During the progression of IVP the pillars increase in number and size, they fuse by folds, and finally lead to complete "cutting-off" of one of the daughter vessels. Importantly, this process that leads to regression of the vasculature takes place at all levels of the vascular bed, from capillary plexus to larger vessels (see Figure 2 and Figure 5).

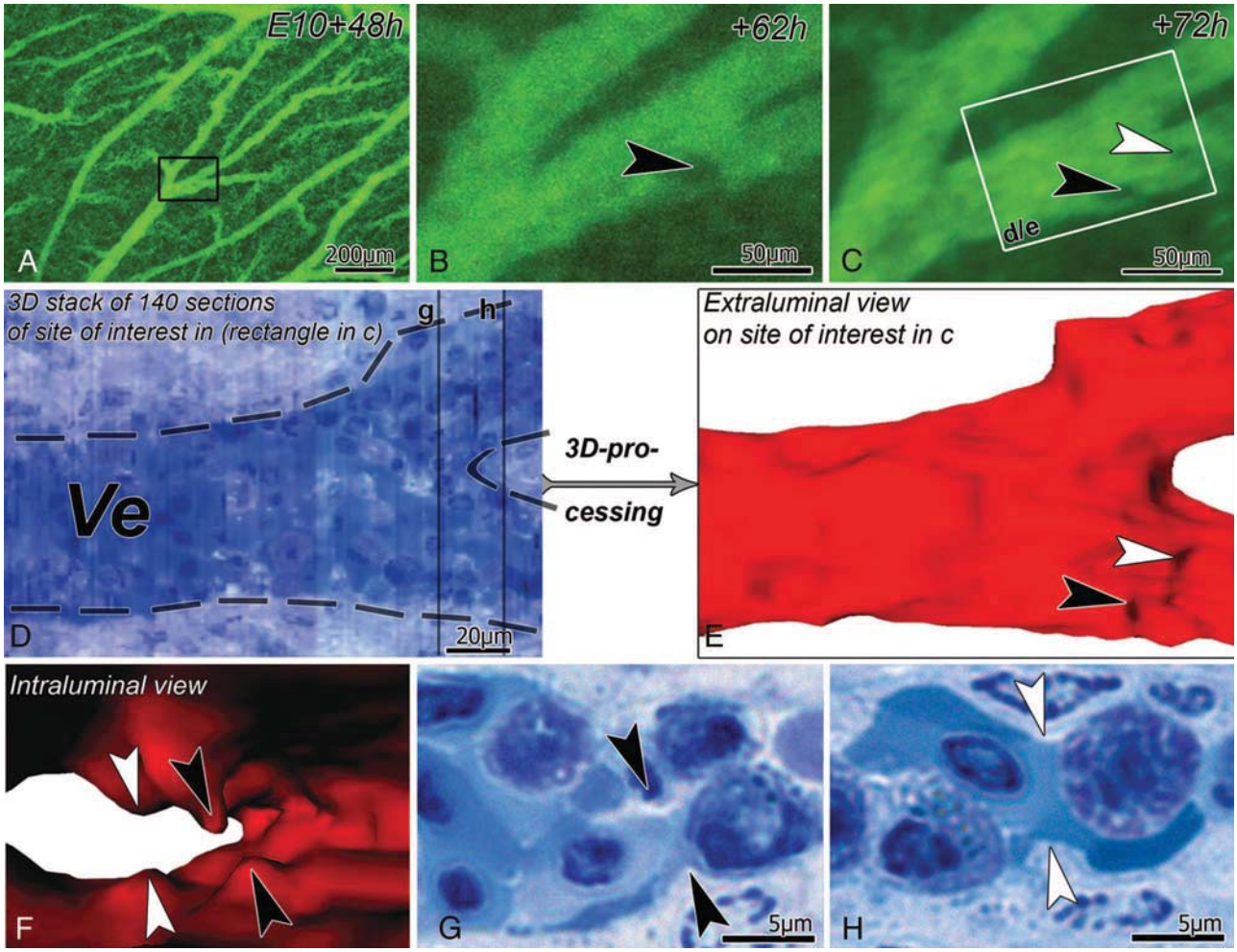

Figure 4. Three dimensional reconstruction of structures observed in vivo. On the overview image (**A**) the site of interest is marked and then presented at higher magnification at later time points (**B**, **C**). At 62 hours after application (**B**) one appearing pillar (black arrowhead) was observed in a supplying vessel, after another 10 hours the second pillar was emerging (white arrowhead in **C**). The site of interest (white rectangle in **C**) was then processed using serial semithin sectioning and the corresponding 3D stack of the images was obtained. The virtual section through this stack is presented in **D** (the contour of the vessel segment [Ve] is marked with the dashed line). The 3D surface of the vascular lumen was generated: **E** shows the overview of the vascular segment of interest with arrowheads indicating the structures corresponding to the ones indicated in **C**. The intraluminal view (**F**) demonstrates the emerging pillars (double arrowheads) at closer distance**.** The lines in **D** mark the position of the toluidine blue-stained semithin sections that are presented in **G** and **H**, showing the emerging pillars (double arrowheads of corresponding color).

VEGF and IVP

VEGF Application Stimulates Angiogenesis in the CAM

In the present study we could observe typical signs of stimulated angiogenesis following application of VEGF-A. It is well described that in addition to the amount of the applied or expressed VEGF, its release modality, ie, slow versus rapid liberation, is a crucial factor for the angiogenic response and vascular morphogenesis.[23–26] Considering the data in the literature, the fibrin gel application was chosen to create an interface between CAM and VEGF-A reservoir and allow a sustained release during the proteolytic degradation of the gel. Microscopical and ELISA-based analysis suggest an exogenous VEGF presentation that lasts for approximately 24 hours after application and that once the gels are completely degraded rapidly terminates. The reversion to the physiological level at 48 hours (on E12) is confirmed by VEGF-ELISA.

VEGF-A Withdrawal Leads to IVP

Although decrease of VEGF concentration has been previously presumed to induce vascular remodeling and pruning,[6,27,28] this hypothesis could only now be affirmed in the present study both qualitatively and quantitatively. Within a rather short time after the decrease of VEGF concentration we observed appearance of many asymmetrically positioned pillars at branching points. Our observations indicate that intussusceptive pillar formation is a major mechanism in VEGF-dependent vascular pruning. This finding is in accordance with other studies describing induction of intussusception and degeneration of immature vessels after inhibition of VEGF-signaling[14,16,29] or hyperoxia-induced withdrawal of VEGF.[30,31] In contrast to the mentioned studies we show here that (VEGF-dependent) IVP is not limited to the immature vasculature but takes places at higher hierarchical levels of the mature vascular bed (see branching of the larger arteries

http://doc.rero.ch

http://doc.rero.ch

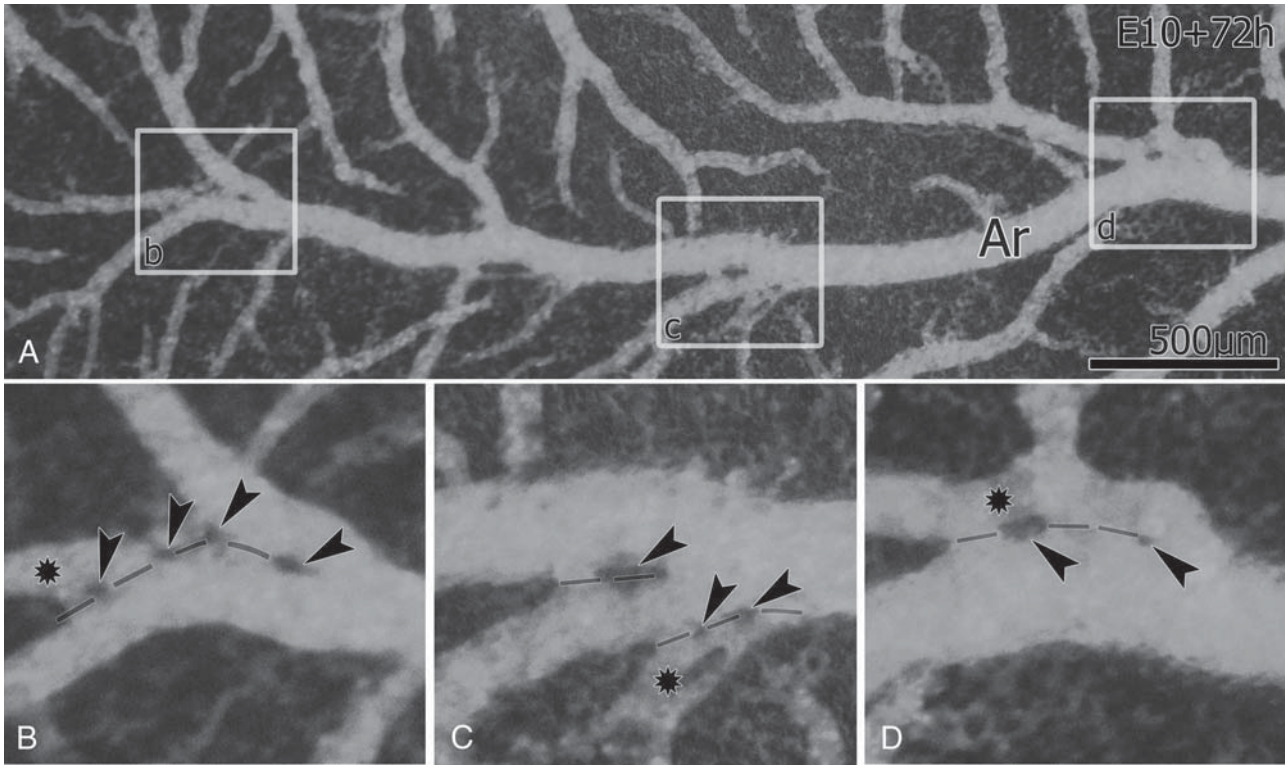

Figure 5. Micrographs from in vivo imaging showing the cascade-like intussusceptive remodeling of the arterial tree after VEGF downregulation. A low magnification image of an artery (Ar) with several branchings is shown in **A**. The branchings undergoing intussusceptive remodeling and pruning (white rectangles in **A**) are displayed at higher magnification in panels **B–D**. The pillars and meshes evident on the vessels (arrowheads in **B–D**) lead to simultaneous IVP and remodeling (dashed lines in **B–D**) at more proximal and distal branching points. This shows the integrity of vascular tree adaptation by means of intussusceptive pruning following vascular endothelial growth factor (VEGF)-A downregulation. The branches separated via IVP are indicated by asterisks in **B–D**. This figure supports the data shown in Fig. 2H that remodeling takes place at different hierarchical levels and is not limited to venous compartment.

in Figure 5). We believe that the IVP of larger mature vessels may be secondary to hemodynamic changes in distal vascular segments, ie, capillary plexus.

There are controversial data in the literature about the fate of the occluded vascular segments. Although most authors postulate that the process involves apoptosis,[16,27,30] pruned ECs may also reassemble into other vessels or dedifferentiate.[32,33] In our model the process of vascular pruning definitely involves apoptosis (Figure 7) but involvement of other mechanisms cannot be excluded.

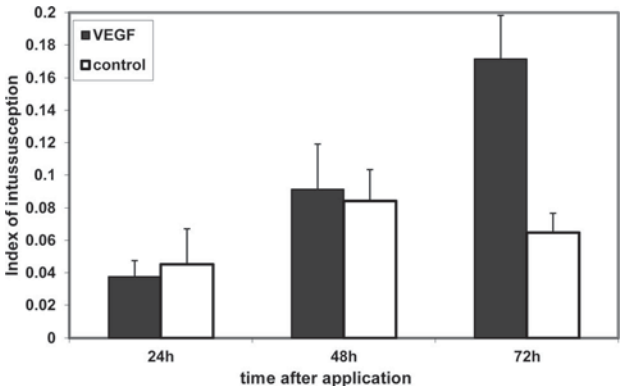

Figure 6. Quantitative evaluation of intussusceptive pruning at branching points. The graph represents the index of intussusception at 24, 48, and 72 hours after vascular endothelial growth factor (VEGF) gel application. The VEGF-A treated areas were characterized by an outstanding increase ($P<0.01$) of the intussusception involvement at 72 hours, at the time-point when VEGF-A expression was already significantly decreased. In the controls there was no significant change between the time-points. The values represented in the graph are mean±SD ($n=4$).

Clinical Implications

Inhibition of angiogenesis is a promising strategy for treatment of cancer and other disorders, whereas promoting growth of new vessels is important for treatment of ischemic disorders. Most antiangiogenic agents in tumor treatment are targeting VEGF signal transduction.[34,35] The antiangiogenic treatment was supposed to deprive the supply of oxygen and nutrients to the tumor by destroying its vasculature. Even a single infusion of bevacizumab, a VEGF-specific antibody, was shown to significantly reduce the microvascular density in rectal carcinoma patients.[36] However, the survival benefits of antiangiogenic drugs have thus far been rather disappointing, stimulating interest in developing more effective ways to combine antiangiogenic drugs with established chemotherapies.[12,37] In the recent past it has been proved that an antiangiogenic approach, when combined with chemotherapy, results in increased survival in patients with advanced malignancies.[8,34] The improved efficacy is nowadays often explained by "vascular normalization." The hypothesis of transient "normalization" of the vasculature states that some antiangiogenic drugs improve tumor perfusion by reducing

http://doc.rero.ch

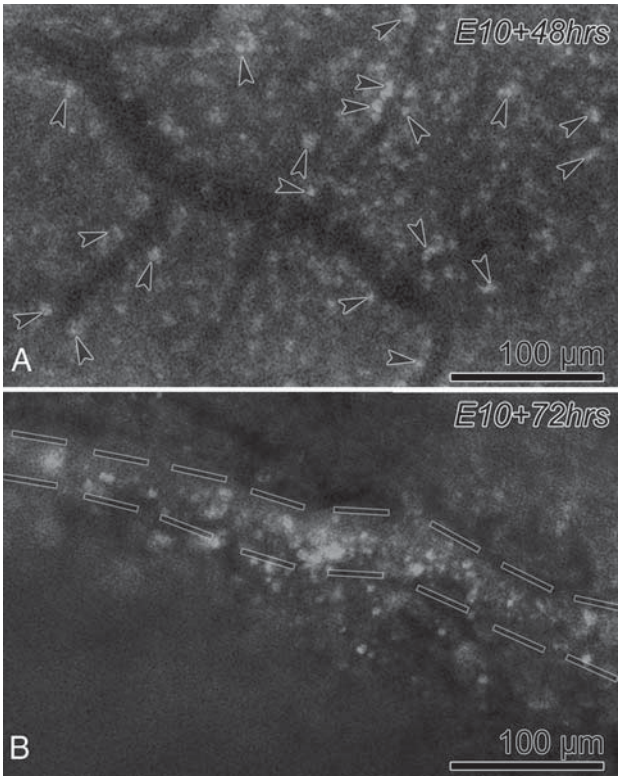

Figure 7. Endothelial cells undergo apoptosis after decline of VEGF concentration. For detection of apoptotic cells the IV injection of FITC-labeled anti-Annexin-V–antibody kit was made prior in vivo observation. At E10+48 hours, (**A**) there were scattered apoptotic cells (arrowheads) in the capillary plexus; at E10+72 hours (**B**) one could observe bigger vessels (contoured with dashed lines) with numerous Annexin-V–positive cells.

vascular density, stabilizing the vessel wall (perivascular cell and basement membrane coverage), reducing the interstitial fluid pressure, and hence increase the penetration of the chemotherapeutic drug into the tumor.[38,39] The underlying morphological mechanisms have not been clearly elucidated yet. In this study we demonstrate for the first time that decrease in VEGF-A concentration leads to intussusceptive remodeling of the vasculature, including pruning. Combined with our previous study on tumor recovery after antiangiogenic treatment this observation may allude to the mechanism underlying the "normalization" of tumor vasculature: VEGF inhibition not only stops further angiogenesis but also leads to transient tumor shrinkage via vascular elimination associated with vessel normalization by activation of IVP and remodeling.

In conclusion, the mechanism of VEGF-dependent IVP described here gives new insights to the understanding of the process of vasculature regression, which is in line with the newer findings of nonsprouting angiogenesis and might provide new potential targets for antiangiogenic therapy.

Acknowledgments

We thank Brigitte Scolari, Clemens Weber, and Regula Buergy for their excellent technical support.

Sources of Funding

This work was supported by Grant No. 3100A0–116243 from the Swiss National Science Foundation.

Disclosures

None.

References

1. Makanya AN, Hlushchuk R, Djonov VG. Intussusceptive angiogenesis and its role in vascular morphogenesis, patterning, and remodeling. *Angiogenesis*. 2009;12:113–123.
2. Franco CA, Liebner S, Gerhardt H. Vascular morphogenesis: a Wnt for every vessel? *Curr Opin Genet Dev*. 2009;19:476–483.
3. Rouget C. Memoire sur le developpement, la structure et les proprietes physiologiques des capillaries sanguins et lymphatiques. *Arch Physiol Norm Pathol*. 1873;5:603–663.
4. Ashton N. Neovascularization in ocular disease. *Trans Ophthalmol Soc UK*. 1961;81:145–161.
5. Ashton N. Oxygen and the growth and development of retinal vessels. In vivo and in vitro studies. The XX Francis I. Proctor Lecture. *Am J Ophthalmol*. 1966;62:412–435.
6. Djonov V, Baum O, Burri PH. Vascular remodeling by intussusceptive angiogenesis. *Cell Tissue Res*. 2003;314:107–117.
7. Risau W. Mechanisms of angiogenesis. *Nature*. 1997;386:671–674.
8. Ferrara N, Kerbel RS. Angiogenesis as a therapeutic target. *Nature*. 2005;438:967–974.
9. Gerber HP, Dixit V, Ferrara N. Vascular endothelial growth factor induces expression of the antiapoptotic proteins Bcl-2 and A1 in vascular endothelial cells. *J Biol Chem*. 1998;273:13313–13316.
10. Ferrara N, Gerber HP, LeCouter J. The biology of VEGF and its receptors. *Nat Med*. 2003;9:669–676.
11. Gerhardt H, Golding M, Fruttiger M, Ruhrberg C, Lundkvist A, Abramsson A, Jeltsch M, Mitchell C, Alitalo K, Shima D, Betsholtz C. VEGF guides angiogenic sprouting utilizing endothelial tip cell filopodia. *J Cell Biol*. 2003;161:1163–1177.
12. Carmeliet P, De SF, Loges S, Mazzone M. Branching morphogenesis and antiangiogenesis candidates: tip cells lead the way. *Nat Rev Clin Oncol*. 2009;6:315–326.
13. Benjamin LE, Hemo I, Keshet E. A plasticity window for blood vessel remodelling is defined by pericyte coverage of the preformed endothelial network and is regulated by PDGF-B and VEGF. *Development*. 1998; 125:1591–1598.
14. Hlushchuk R, Riesterer O, Baum O, Wood J, Gruber G, Pruschy M, Djonov V. Tumor recovery by angiogenic switch from sprouting to intussusceptive angiogenesis after treatment with PTK787/ZK222584 or ionizing radiation. *Am J Pathol*. 2008;173:1173–1185.
15. Shweiki D, Itin A, Soffer D, Keshet E. Vascular endothelial growth factor induced by hypoxia may mediate hypoxia-initiated angiogenesis. *Nature*. 1992;359:843–845.
16. Hlushchuk R, Baum O, Gruber G, Wood J, Djonov V. The synergistic action of a VEGF-receptor tyrosine-kinase inhibitor and a sensitizing PDGF-receptor blocker depends upon the stage of vascular maturation. *Microcirculation*. 2007;14:813–825.
17. Ehrbar M, Rizzi SC, Schoenmakers RG, Miguel BS, Hubbell JA, Weber FE, Lutolf MP. Biomolecular hydrogels formed and degraded via site-specific enzymatic reactions. *Biomacromolecules*. 2007;8:3000–3007.
18. Djonov V, Schmid M, Tschanz SA, Burri PH. Intussusceptive angiogenesis: its role in embryonic vascular network formation. *Circ Res*. 2000;86:286–292.
19. Djonov VG, Kurz H, Burri PH. Optimality in the developing vascular system: branching remodeling by means of intussusception as an efficient adaptation mechanism. *Dev Dyn*. 2002;224:391–402.
20. Ehrbar M, Zeisberger SM, Raeber GP, Hubbell JA, Schnell C, Zisch AH. The role of actively released fibrin-conjugated VEGF for VEGF receptor 2 gene activation and the enhancement of angiogenesis. *Biomaterials*. 2008;29:1720–1729.
21. Augustin H. *Methods in Endothelial Cell Biology*. Berlin: Springer; 2004.
22. Burri PH, Hlushchuk R, Djonov V. Intussusceptive angiogenesis: its emergence, its characteristics, and its significance. *Dev Dyn*. 2004;231: 474–488.
23. Auerbach R, Lewis R, Shinners B, Kubai L, Akhtar N. Angiogenesis assays: a critical overview. *Clin Chem*. 2003;49:32–40.
24. Ehrbar M, Djonov VG, Schnell C, Tschanz SA, Martiny-Baron G, Schenk U, Wood J, Burri PH, Hubbell JA, Zisch AH. Cell-demanded liberation of VEGF121 from fibrin implants induces local and controlled blood vessel growth. *Circ Res*. 2004;94:1124–1132.
25. Hagedorn M, Balke M, Schmidt A, Bloch W, Kurz H, Javerzat S, Rousseau B, Wilting J, Bikfalvi A. VEGF coordinates interaction of

pericytes and endothelial cells during vasculogenesis and experimental angiogenesis. *Dev Dyn*. 2004;230:23–33.
26. Wilting J, Birkenhager R, Eichmann A, Kurz H, Martiny-Baron G, Marme D, McCarthy JE, Christ B, Weich HA. VEGF121 induces proliferation of vascular endothelial cells and expression of flk-1 without affecting lymphatic vessels of chorioallantoic membrane. *Dev Biol*. 1996; 176:76–85.
27. Dor Y, Djonov V, Abramovitch R, Itin A, Fishman GI, Carmeliet P, Goelman G, Keshet E. Conditional switching of VEGF provides new insights into adult neovascularization and pro-angiogenic therapy. *EMBO J*. 2002; 21:1939–1947.
28. Dor Y, Porat R, Keshet E. Vascular endothelial growth factor and vascular adjustments to perturbations in oxygen homeostasis. *Am J Physiol Cell Physiol*. 2001;280:C1367–C1374.
29. Jain RK, Duda DG, Clark JW, Loeffler JS. Lessons from phase III clinical trials on anti-VEGF therapy for cancer. *Nat Clin Pract Oncol*. 2006;3: 24–40.
30. Alon T, Hemo I, Itin A, Pe'er J, Stone J, Keshet E. Vascular endothelial growth factor acts as a survival factor for newly formed retinal vessels and has implications for retinopathy of prematurity. *Nat Med*. 1995;1: 1024–1028.
31. Lange C, Ehlken C, Stahl A, Martin G, Hansen L, Agostini HT. Kinetics of retinal vaso-obliteration and neovascularisation in the oxygen-induced retinopathy (OIR) mouse model. *Graefes Arch Clin Exp Ophthalmol*. 2009;247:1205–1211.
32. Markwald RR, Krug EL, Mjaatvedt CH, Sinning AR. Endothelial formation of mesenchyme: Induction by an extracellular glycoprotein complex. In: Robertson R and Schneider MD, ed. *Molecular biology of the cardiovascular system.* 1990;311–319.
33. Feinberg RN, Noden DM. Experimental analysis of blood vessel development in the avian wing bud. *Anat Rec*. 1991;231:136–144.
34. Bergers G, Hanahan D. Modes of resistance to anti-angiogenic therapy. *Nat Rev Cancer*. 2008;8:592–603.
35. Furuya M, Yonemitsu Y, Aoki I, III. Angiogenesis: complexity of tumor vasculature and microenvironment. *Curr Pharm Des*. 2009;15: 1854–1867.
36. Willett CG, Boucher Y, di Tomaso E, Duda DG, Munn LL, Tong RT, Chung DC, Sahani DV, Kalva SP, Kozin SV, Mino M, Cohen KS, Scadden DT, Hartford AC, Fischman AJ, Clark JW, Ryan DP, Zhu AX, Blaszkowsky LS, Chen HX, Shellito PC, Lauwers GY, Jain RK. Direct evidence that the VEGF-specific antibody bevacizumab has antivascular effects in human rectal cancer. *Nat Med*. 2004;10:145–147.
37. Ma J, Waxman DJ. Combination of antiangiogenesis with chemotherapy for more effective cancer treatment. *Mol Cancer Ther*. 2008;7: 3670–3684.
38. Jain RK. Normalization of tumor vasculature: an emerging concept in antiangiogenic therapy. *Science*. 2005;307:58–62.
39. Tong RT, Boucher Y, Kozin SV, Winkler F, Hicklin DJ, Jain RK. Vascular normalization by vascular endothelial growth factor receptor 2 blockade induces a pressure gradient across the vasculature and improves drug penetration in tumors. *Cancer Res*. 2004;64:3731–3736.

http://doc.rero.ch

http://doc.rero.ch

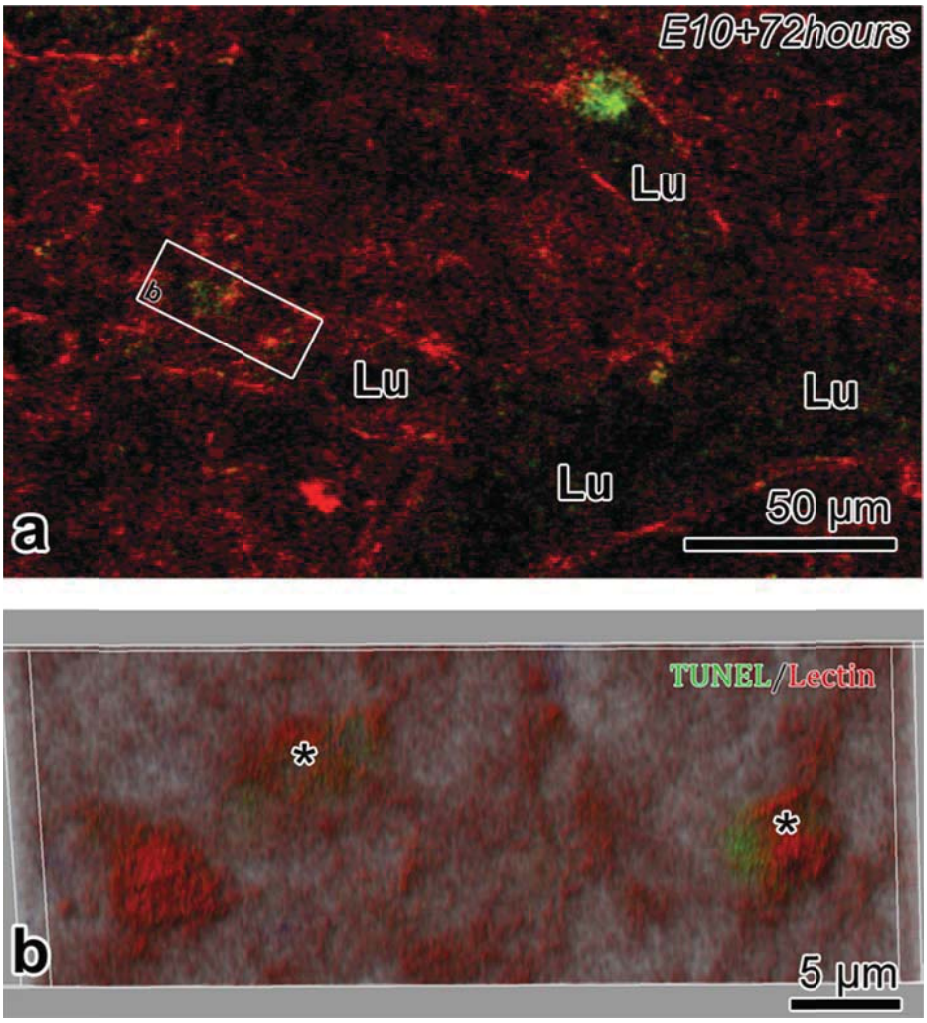

Supplemental Figure 1. Verification of the apoptosis of ECs by the investigation of doubled stained (TUNEL and lectin) whole-mount samples harvested at 72 hours after the VEGF application in LSM Zeiss 510 M. The overview picture (a) displays the cross-section through the whole-mount sample with apparent vascular lumen (Lu). The projection image ("Volume") of a Z-stack of LSM images of endothelial vascular surface (red=endothelial cell surface marker) distinctly shows TUNEL-positive (green) endothelial cells. Nuclei of apoptotic endothelial cells are indicated with *asterisks*.

Material and method:

Apoptosis (TUNEL) assay combined with endothelial cell surface staining

The whole–mount samples of the CAM vasculature were harvested and fixed in 2%PFA at 72 hours after the VEGF gel application. They were further stained for fluorescence staining using the TUNEL Label Mix (Roche Diagnostics AG, Switzerland; Cat Nr:11767291910) to visualize the apoptotic cells and rhodamine-labeled Lens culinaris agglutinin (LCA) (Vector Labs, CA, USA; Cat. Nr: RL-1042) for visualization of endothelial cell surface according to the manufacturer's recommendations. The mounted samples were then investigated in the LSM Zeiss 510M, the obtained Z-stacks of images were afterwards imported in and analysed by Imaris Software.

Downloaded from http://atvb.ahajournals.org/ at Bibliothèque Cantonale et Universitaire de Fribourg on January 24, 2012